

Local photodoping in monolayer MoS₂

Andreij C. Gadelha,¹ Alisson R. Cadore,^{1,2} Lucas Lafeta,¹ Ana M. de Paula,¹
Leandro M. Malard,¹ Rodrigo G. Lacerda,¹ and Leonardo C. Campos¹

¹*Departamento de Física, Universidade Federal de Minas Gerais, Belo Horizonte, MG 31270-901, Brasil*

²*Cambridge Graphene Centre, University of Cambridge, Cambridge CB3 0FA, United Kingdom*

Abstract

Inducing electrostatic doping in 2D materials by laser exposure (photodoping effect) is an exciting route to tune optoelectronic phenomena. However, there is a lack of investigation concerning in what respect the action of photodoping in optoelectronic devices is local. Here, we employ scanning photocurrent microscopy (SPCM) techniques to investigate how a permanent photodoping modulates the photocurrent generation in MoS₂ transistors locally. We claim that the photodoping fills the electronic states in MoS₂ conduction band, preventing the photon-absorption and the photocurrent generation by the MoS₂ sheet. Moreover, by comparing the persistent photocurrent (PPC) generation of MoS₂ on top of different substrates, we elucidate that the interface between the material used for the gate and the insulator (gate-insulator interface) is essential for the photodoping generation. Our work gives a step forward to the understanding of the photodoping effect in MoS₂ transistors and the implementation of such an effect in integrated devices.

Introduction

Two-dimensional (2D) materials are strategically important for optoelectronic applications due to their ultra-thin nature and tunable electrostatic and optical properties [1–12]. Among all layered materials [13], the vast family of the transition metal dichalcogenides (TMDCs) has particular significance because many of these materials are direct band gap 2D semiconductors in the monolayer form [2], bringing light to interesting valleytronic properties [9–11], high photoluminescence emission [14], and high photocurrent response [3–7]. Furthermore, many paths have been proposed to tune the optoelectronic properties of TMDCs, including strain engineering [15–17], electric and magnetic fields applications [18, 19], and more recently integrating TMDC monolayers in twisted heterostructures [20, 21]. In special, using laser exposure to modulate the density of charge in 2D materials, also called by photodoping effect, has emerged as a convenient way to engineer optoelectronic devices [8, 12, 22–33]. For instance, photodoping has been used to generate p-n junctions in graphene [29], for applications in photovoltaics using WSe₂ [33], to enhance the optoelectronic performance of WS₂ [27], to demonstrate a gate-tunable photomemory effect [8], and to propose alternative optical memory devices [12, 32–34]. However, there is a lack of information regarding how photodoping modifies TMDCs in a locally and controllable fashion.

Here we investigate the local modification of MoS₂ photocurrent due to the photodoping effect in a monolayer MoS₂ on top of SiO₂/Si transistor. We demonstrate photodoping as high as $\Delta n_{\text{ph}} = 8.5 \times 10^{12} \text{ cm}^{-2}$ in MoS₂ just by laser exposure and gate-voltage applications. Also, temporal analysis of the photodoping suggests that it is a permanent doping, retaining up to 77 % of the initial photodoping. Besides, we use a scanning photocurrent microscopy setup (SPCM) that gives information about the photodoping effect with a resolution limited by the spot area of the laser (approximately $1 \mu\text{m}^2$ in our setup). Then, we show that the photodoping is a local effect and inhibits photocurrent in specific local regions of monolayer MoS₂. Finally, we study the persistent photocurrent (PPC) in the MoS₂ sheet placed in different substrates, and we point out that the gate-insulator interface is crucial for the photodoping generation. In summary, our work expands the possibilities of controlling the optoelectronic properties of 2D materials.

Results and Discussion

Fig. 1(a) shows a sketch of the device that we study in this work. The device is a MoS₂ field-effect transistor (FET) composed of a monolayer MoS₂ on a SiO₂/Si substrate, where we use a highly n-type doped Si wafer as a back gate terminal [35]. We do all the measurements in a vacuum ($P \approx 10^{-6}$ mbar) and at room temperature. Fig. 1(b) shows a map of the intensity of the MoS₂ photoluminescence centered in $\lambda = 680$ nm and with an excitation wavelength of $\lambda = 457$ nm, demonstrating that the monolayer MoS₂ sheet is uniform. To measure the photodoping, we compare transfer curves, current (I_{SD}) vs back gate voltage (V_{BG}) curves, before and after the laser exposure, see Fig. 1(c).

In blue, Fig. 1(c), we plot a transfer curve before the laser exposure. We estimate the threshold voltage (V_{th}) as $V_{th}^0 = -14$ V by extrapolating the I_{SD} curve. Then, we expose the MoS₂ device to the laser $\lambda = 488$ nm with $V_{BG} = -50$ V until the photocurrent saturates. Next, we turn the laser off and repeat the measurement to evaluate the transfer curve. The data from the transfer curve after the laser exposure (red curve in Fig. 1(c)) exhibits a significant increase of I_{SD} for all applied gate conditions. A shift of V_{th} in the experiment causes the increasing behavior of I_{SD} , a signature of photodoping effect [8, 29]. Hence, the photodoping effect is a consequence of a change on the density of free charges of MoS₂ promoted by the laser exposure. We estimate that the initial $V_{th}^0 = -14$ V shifts to $V_{th}^L = -127$ V after laser exposure, see Fig. 1(c), resulting in a change in the density of charge of MoS₂ of $\Delta n_{ph} = 8.5 \times 10^{12}$ cm⁻², which is evaluated using the equation:

$$\Delta n_{ph} = \frac{\varepsilon_0 \varepsilon_{ox}}{e d} (V_{th}^L - V_{th}^0) \quad (1)$$

where ε_{ox} and d are the dielectric constant of the insulator and its thickness, respectively. Note that such extra doping is obtained simply by the combination of laser exposure and the applied gate bias.

To exploit the photodoping effect in robust integrated devices, they must hold the photodoping for long periods [32]. To assess this issue, we measure the MoS₂ photodoping time dependency, see the black dots in Fig. 1(d). In this case, we evaluate the photodoping by measuring the MoS₂ photocurrent applying $V_{SD} = 1$ V and $V_{BG} = 0$ V, and using formula $\Delta n_{ph} = \Delta \sigma_{ph} / e \mu$, where $\Delta \sigma_{ph}$ is the photoconductance and μ is the mobility of the device. We measure the decay of the photodoping following the saturation of the photocur-

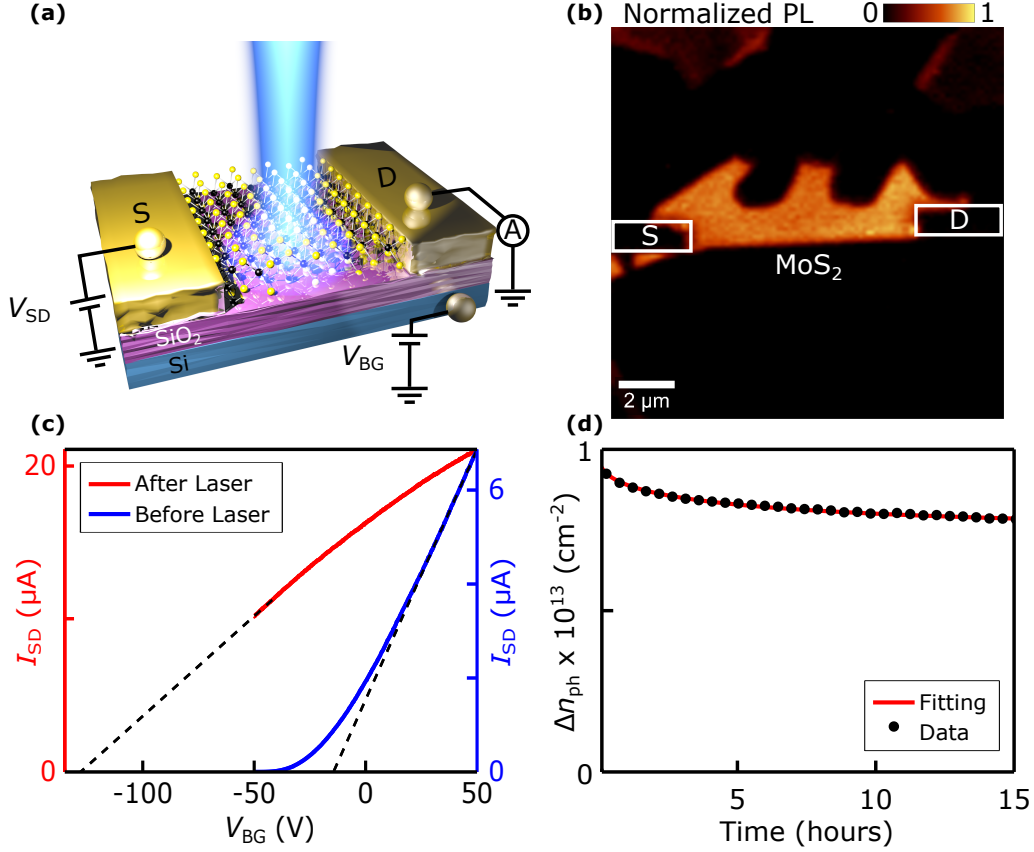


FIG. 1. **Photodoping in MoS₂**. (a), sketch of the MoS₂ FET. (b), normalized photoluminescence image from the integrated area of the intensity of the maximum photoluminescence peak of MoS₂. This measurement is done with a 457 nm laser, 1 μm spot size and power density of 340 $\mu\text{W}/\mu\text{m}^2$. (c), the I_{SD} vs V_{BG} measurements before (blue) and after (red) the laser exposure, $V_{\text{SD}} = 1\text{ V}$. The red curve is measured after the 488 nm laser exposure with a power density of 700 $\mu\text{W}/\mu\text{m}^2$ and $V_{\text{BG}} = -50\text{ V}$ until photocurrent saturation. (d), photocurrent decay after the photodoping induced by the 488 nm laser with a power density of 700 $\mu\text{W}/\mu\text{m}^2$ until photocurrent saturation. The parameters $V_{\text{BG}} = 0\text{ V}$ and $V_{\text{SD}} = 1\text{ V}$ are used for this measurement.

rent by laser exposure. After 15 h, the photodoping barely decreases, suggesting that the photodoping effect is permanent. To provide an estimative for the photodoping loss over a long period, we employ an exponential decay fit, the red line in Fig. 1(d). From the fitting, we predict that the reminiscent photodoping is approximately 77% of its initial value. Thus, the devices can retain 77% of the charge induced by the laser permanently, which is ideal for their integration in optoelectronic circuits.

We now show that the photodoping is a local effect by the spatial control of the photocur-

rent generation in MoS₂, see Fig. 2. To visualize the spatial distribution of photodoping, we use an SPCM setup. SPCM is a useful tool to investigate local optoelectronic effects and have been used to elucidate the photocurrent in MoS₂ [36], to observe photothermoelectric effect in both graphene and MoS₂ [37, 38] and to image a p-n junction in graphene [29]. The photodoping generation is a relatively slow process because the laser induces typical dopings of $\Delta n_{\text{ph}} \approx 10^{12} \text{ cm}^{-2}$ after an exposure time of 10 s in a single point [8]. On the other hand, the SPCM measures photocurrents with fast response time (\approx ms) solely. We support this statement on the SPCM setup, where the laser intensity is modulated at 3 kHz with an optical chopper, generating an alternating photocurrent signal in MoS₂. Subsequently, a lock-in, synchronized with the chopper, filters this alternating signal, preventing the observation of photocurrents with a response time higher than \approx ms. Hence, the SPCM does not measure the photodoping, which is a slow process, directly. What we observe in an SPCM image is predominantly the photocurrent due to the generation of electron-hole pairs in MoS₂, which have a typical photocurrent response time of \approx ms [36, 39]. However, we show that we can distinguish photodoping in SPCM images indirectly, see Fig. 2. Fig. 2(a) shows a SPCM measurement for the MoS₂ device using a 561 nm (2.2 eV) laser with a power density of $100 \mu\text{W}/\mu\text{m}^2$. A gate voltage of -70 V is applied in MoS₂ while the measurement is performed to ensure that the sample is almost depleted of charges.

During the SPCM measurement, the laser dwells at each point for small periods ($\tau \approx 500 \text{ ms}$), which generates a small ($\Delta n_{\text{ph}} \approx 10^{11} \text{ cm}^{-2}$) photodoping in the whole sample. To prevent distortions in the SPCM images due to the small photodoping generation during the SPCM measurement, we normalize all the measurements of Fig. 2 with the photocurrent from the region indicated by the arrow. We show in Fig. 2(b) the band structure near the band edges for the delineated region by the dashed circle (see Fig. 2(a)) in order to understand the physical mechanism of the photocurrent generation in Fig. 2(a). Since the sample is almost depleted with charges, the sample absorbs some photons that excite electrons from the valence to the conduction band generating an excess of carriers [5, 36]. Afterward, the photogenerated excess of carriers becomes a photocurrent by the applied bias [5, 36]. Indeed, the photocurrent is generated throughout the sample, see Fig. 2(a), but higher values are attained close to the contact interface due to Schottky electric field [36].

After measuring the photocurrent spatially, we expose the delimited area (dashed circle) in Fig. 2(a) with the 561 nm laser with a power density of $1000 \mu\text{W}/\mu\text{m}^2$ and $V_{\text{BG}} = -50 \text{ V}$

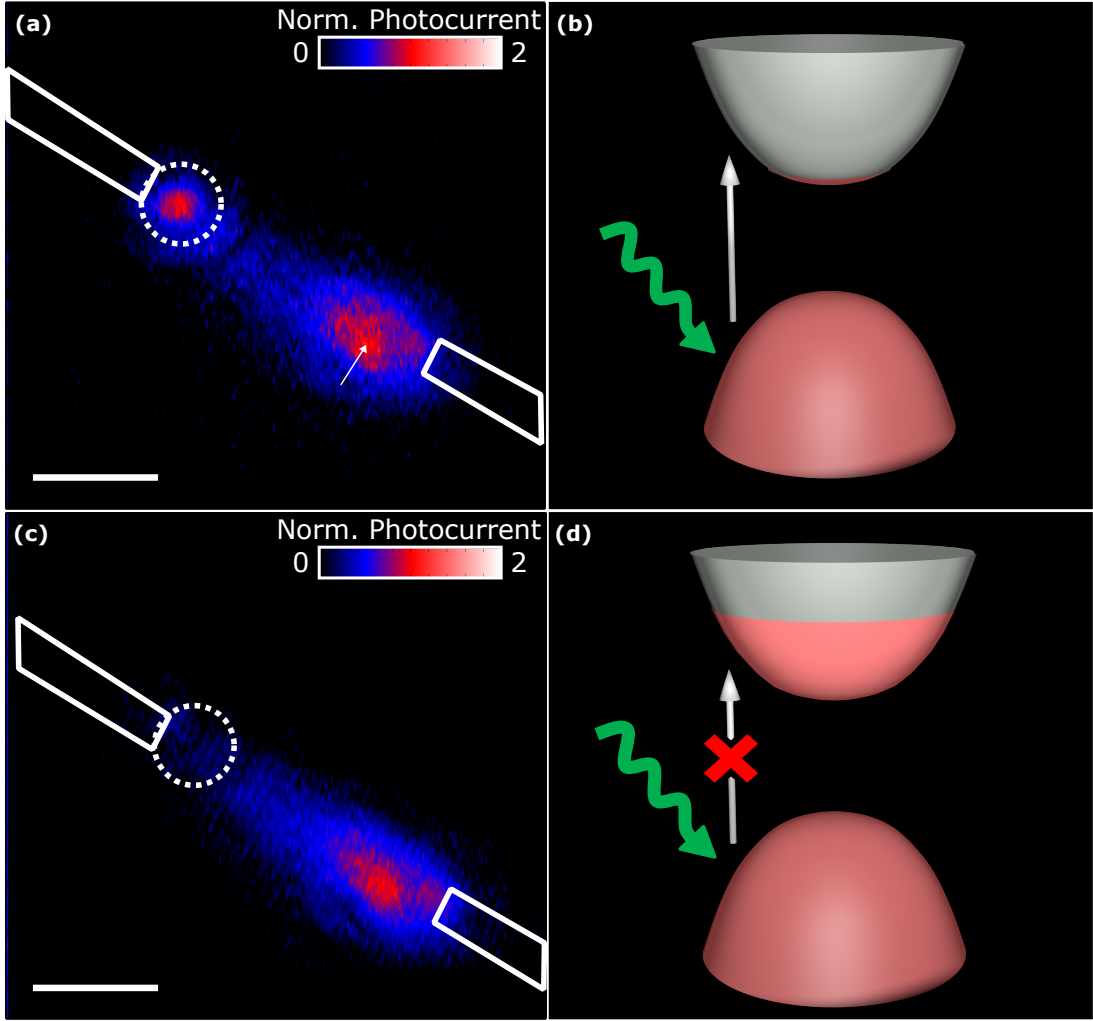


FIG. 2. **Spatial control of the photocurrent.** (a), scanning photocurrent microscopy measurement for the MoS₂/SiO₂ sample. The excitation laser wavelength is 561 nm with a power density of 100 $\mu\text{W}/\mu\text{m}^2$. In this measurement we use $V_{\text{BG}} = -70$ V and $V_{\text{SD}} = 1$ V. (b), the band structure of the region inside the dashed circle in panel (a). (c), SPCM measurement from the same region and conditions as in (a), but after exposing the region inside the dashed circle in panel (a) with the $\lambda = 561$ nm laser, power density of 1000 $\mu\text{W}/\mu\text{m}^2$ and $V_{\text{BG}} = -50$ V for five minutes. (d), the band structure of the region inside the dashed circle in panel (c). Scale bar is 4 μm .

for five minutes to ensure that a photodoping is generated. After that, we repeat the SPCM measurement with the same parameters used in Fig. 2(a), and suppression of the photocurrent occurs in the exposed region, as shown in Fig. 2(c). We explain this local effect qualitatively via a photodoping process. Fig. 2(d) depicts the band diagram of MoS₂ in the dashed circle area that shows why the photocurrent is suppressed. After inducing the

photodoping in the dashed area, the states in the conduction band are filled, which limits the photoexcitation of electron-hole pairs [3]. Thus, there is a suppression of the photocurrent in the exposed area (see Fig. 2(c)), indicating that the photodoping effect controls locally the photocurrent in the MoS₂ channel.

Now, we show that interactions with the gate-insulator interface impact the photodoping generation process. We propose in reference [8] a model that claims the physics of the photodoping effect is contained mostly in the gate-insulator interface. As the gate-insulator interface is crucial for the photodoping generation [8], we predict that devices that do not have a gate-insulator interface do not generate photodoping. To evaluate this point experimentally, we compare the photodoping generation of two devices, with and without a gate terminal, keeping the same insulator as the substrate, see Fig. 3. The simplest way to prepare these devices is by using a standard MoS₂ FET on a SiO₂/Si substrate (SiO₂/Si device), and by using a MoS₂ sample on top of glass (SiO₂ device). So, the first device has a gate electrode, whereas the second one does not, while both have the same insulator substrate (SiO₂). Fig. 3(a) shows a I_{SD} vs Time curve of the SiO₂/Si device, and in the inset we show a sketch of this device. In Fig. 3(a), we initially measure the current of the device in dark conditions, then we turn the laser on ($\lambda = 488$ nm) for approximately 25 s.

By analyzing the time dependence of current (Fig. 3(a)), we point out two optical processes that are generating the photocurrent in the MoS₂ channel, see Fig. 3(a). First, we observe a rapid enhance of I_{SD} due to excitation of electron-hole pairs (see vertical red arrow), followed by a second and slow process that keeps increasing the photocurrent with time. A similar trend, but with decreasing photocurrent occurs when the laser is turned off, there is a fast reduction of I_{SD} , due to the recombination of electron-hole pairs, succeed by a slow decay process that leads to a PPC. In reference [8], we argued that the photodoping effect causes the PPC, and here we show experimentally that the gate-insulator interface is essential for the photodoping generation. To elaborate on this issue, we analyze the photocurrent generation in the SiO₂ device. Fig. 3(b) shows an I_{SD} vs Time curve of the SiO₂ device, while the inset shows a sketch of this device. In contrast to the response of the SiO₂/Si device, the SiO₂ device presents a very sharp and fast response. Thus, the SiO₂ device, which does not have a gate-insulator interface, presents negligible PPC. So, the choice of the substrate interface in a MoS₂ device is decisive to the observation of a PPC, as reported in previous experiments [40].

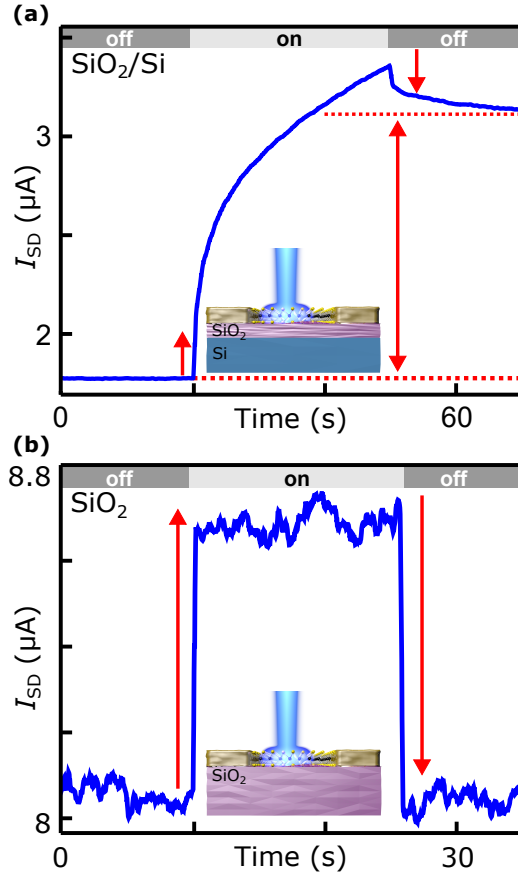


FIG. 3. **Photodoping and the gate-insulator interface.** (a), time-resolved photocurrent for the SiO₂/Si device, $V_{BG}=0$ V. In the inset, sketch of the SiO₂/Si device. (b), time-resolved photocurrent for the SiO₂ device. In the inset, sketch of the SiO₂ device. In both measurements we use a 488 nm laser with a power density of $60 \mu\text{W}/\mu\text{m}^2$.

Conclusion

In conclusion, we showed that a high permanent photodoping could be attained in MoS₂ transistors only by laser exposure and applied gate voltage. We used an SPCM setup to demonstrate that the photodoping effect controls the photocurrent generation spatially in the MoS₂ transistor. Moreover, we showed that the photodoping mechanism is only present in devices with a gate-insulator interface. Therefore our work opens up possibilities to use the local photodoping in novel optoelectronic devices and to engineer the gate-insulator interface in order to control the photodoping mechanism.

Methods

Device Fabrication. The SiO_2/Si device was obtained from direct exfoliation of MoS_2 on a Si wafer with a 285 nm thick silicon oxide. Metal leads were patterned by electron-beam lithography and subsequent deposition of metals (Au 50 nm). The *si* device was obtained by depositing the metals first (Cr 1 nm/Au 50 nm) on a glass substrate. Then MoS_2 flakes were transferred to this structure by dry viscoelastic stamping technique [41].

Optoelectronic Measurements. To provide a source-drain bias the external DC source of a standard lock-in amplifier (SR830) was used. While to provide a gate bias a Keithley 2400 were used. The current of the devices was collected by a pre-amplifier and then measured by a multimeter (Keithley 2000). To generate the photocurrent in the MoS_2 FET a 488 nm laser beam was focused in the devices by a $50\times$ objective lens ($\sim 1\ \mu\text{m}$ spotsize). For SPCM measurements, a 561 nm laser beam was directed to a chopper working at 3000 Hz and then focused on the device by a $50\times$ objective lens. The MoS_2 alternate photocurrent was collected by the pre-amplifier and the signal was measured by the lock-in amplifier

Acknowledgments

This work was supported by CAPES, Fapemig (Rede 2D), CNPq, Rede de Nano-Instrumentação, and INCT/Nanomaterials de Carbono. The authors are thankful to the Laboratory of Nano Spectroscopy at UFMG for providing an experimental setup for this work, and to Centro Brasileiro de Pesquisas Físicas (CBPF) and Centro de Componentes Semicondutores (CCS) for providing an e-beam lithography system and the Lab Nano at UFMG for allowing the use of an atomic force microscope.

Competing financial interests

The authors declare no competing financial interests

References

- [1] B. Radisavljevic, A. Radenovic, J. Brivio, V. Giacometti, and A. Kis. Single-layer MoS₂ transistors. *Nat Nano*, 6(3):147–150, March 2011.
- [2] Sajedeh Manzeli, Dmitry Ovchinnikov, Diego Pasquier, Oleg V. Yazyev, and Andras Kis. 2D transition metal dichalcogenides. *Nature Reviews Materials*, 2:17033–, June 2017.
- [3] Oriol Lopez-Sanchez, Dominik Lembke, Metin Kayci, Aleksandra Radenovic, and Andras Kis. Ultrasensitive photodetectors based on monolayer MoS₂. *Nat Nano*, 8(7):497–501, July 2013.
- [4] M. F. Khan, M. W. Iqbal, M. Z. Iqbal, M. A. Shehzad, Y. Seo, and Jonghwa Eom. Photocurrent response of MoS₂ field-effect transistor by deep ultraviolet light in atmospheric and N₂ gas environments. *ACS Applied Materials & Interfaces*, 6(23):21645–21651, 2014. PMID: 25409490.
- [5] Zongyou Yin, Hai Li, Hong Li, Lin Jiang, Yumeng Shi, Yinghui Sun, Gang Lu, Qing Zhang, Xiaodong Chen, and Hua Zhang. Single-layer MoS₂ phototransistors. *ACS Nano*, 6(1):74–80, 2012. PMID: 22165908.
- [6] Woong Choi, Mi Yeon Cho, Aniruddha Konar, Jong Hak Lee, Gi-Beom Cha, Soon Cheol Hong, Sangsig Kim, Jeongyong Kim, Debdeep Jena, Jinsoo Joo, and Sunkook Kim. High-detectivity multilayer MoS₂ phototransistors with spectral response from ultraviolet to infrared. *Advanced Materials*, 24(43):5832–5836, 2012.
- [7] Riccardo Frisenda, Aday J. Molina-Mendoza, Thomas Mueller, Andres Castellanos-Gomez, and Herre S. J. van der Zant. Atomically thin p-n junctions based on two-dimensional materials. *Chem. Soc. Rev.*, 47(9):3339–3358, 2018.
- [8] Andreij C Gadelha, Alisson R Cadore, Kenji Watanabe, Takashi Taniguchi, Ana M de Paula, Leandro M Malard, Rodrigo G Lacerda, and Leonardo C Campos. Gate-tunable non-volatile photomemory effect in MoS₂ transistors. *2D Materials*, 6(2):025036, mar 2019.
- [9] K. F. Mak, K. L. McGill, J. Park, and P. L. McEuen. The valley hall effect in MoS₂ transistors. *Science*, 344(6191):1489–1492, 2014.
- [10] Christian Schneider, Mikhail M. Glazov, Tobias Korn, Sven Höfling, and Bernhard Urbaszek. Two-dimensional semiconductors in the regime of strong light-matter coupling. *Nature Communications*, 9(1):2695–, 2018.

-
- [11] Nils Lundt, Lukasz Dusanowski, Evgeny Sedov, Petr Stepanov, Mikhail M. Glazov, Sebastian Klembt, Martin Klaas, Johannes Beierlein, Ying Qin, Sefaattin Tongay, Maxime Richard, Alexey V. Kavokin, Sven Höfling, and Christian Schneider. Optical valley hall effect for highly valley-coherent exciton-polaritons in an atomically thin semiconductor. *Nature Nanotechnology*, 14(8):770–775, 2019.
- [12] Juwon Lee, Sangyeon Pak, Young-Woo Lee, Yuljae Cho, John Hong, Paul Giraud, Hyeon Suk Shin, Stephen M. Morris, Jung Inn Sohn, SeungNam Cha, and Jong Min Kim. Monolayer optical memory cells based on artificial trap-mediated charge storage and release. *Nature Communications*, 8:14734–, March 2017.
- [13] Nicolas Mounet, Marco Gibertini, Philippe Schwaller, Davide Campi, Andrius Merkys, Antimo Marrazzo, Thibault Sohier, Ivano Eligio Castelli, Andrea Cepellotti, Giovanni Pizzi, and Nicola Marzari. Two-dimensional materials from high-throughput computational exfoliation of experimentally known compounds. *Nature Nanotechnology*, 13(3):246–252, 2018.
- [14] Hyungjin Kim, Geun Ho Ahn, Joy Cho, Matin Amani, James P. Mastandrea, Catherine K. Groschner, Der-Hsien Lien, Yingbo Zhao, Joel W. Ager, Mary C. Scott, Daryl C. Chrzan, and Ali Javey. Synthetic WSe₂ monolayers with high photoluminescence quantum yield. *Science Advances*, 5(1), 2019.
- [15] Zhaohe Dai, Luqi Liu, and Zhong Zhang. 2D materials: Strain engineering of 2D materials: Issues and opportunities at the interface (adv. mater. 45/2019). *Advanced Materials*, 31(45):1970322, 2019.
- [16] Carmen Palacios-Berraquero, Dhiren M. Kara, Alejandro R.-P. Montblanch, Matteo Barbone, Pawel Latawiec, Duhee Yoon, Anna K. Ott, Marko Loncar, Andrea C. Ferrari, and Mete Atatüre. Large-scale quantum-emitter arrays in atomically thin semiconductors. *Nature Communications*, 8(1):15093–, 2017.
- [17] Patricia Gant, Peng Huang, David Péez de Lara, Dan Guo, Riccardo Frisenda, and Andres Castellanos-Gomez. A strain tunable single-layer MoS₂ photodetector. *Materials Today*, 27:8 – 13, 2019.
- [18] Zhipeng Li, Tianmeng Wang, Chenhao Jin, Zhengguang Lu, Zhen Lian, Yuze Meng, Mark Blei, Shiyuan Gao, Takashi Taniguchi, Kenji Watanabe, Tianhui Ren, Sefaattin Tongay, Li Yang, Dmitry Smirnov, Ting Cao, and Su-Fei Shi. Emerging photoluminescence from the dark-exciton phonon replica in monolayer WSe₂. *Nature Communications*, 10(1):2469–, 2019.

-
- [19] Matteo Barbone, Alejandro R.-P. Montblanch, Dhiren M. Kara, Carmen Palacios-Berraquero, Alisson R. Cadore, Domenico De Fazio, Benjamin Pingault, Elaheh Mostaani, Han Li, Bin Chen, Kenji Watanabe, Takashi Taniguchi, Sefaattin Tongay, Gang Wang, Andrea C. Ferrari, and Mete Atatüre. Charge-tuneable biexciton complexes in monolayer WSe₂. *Nature Communications*, 9(1):3721–, 2018.
- [20] Xiaobo Lu, Xiaoqin Li, and Li Yang. Modulated interlayer exciton properties in a two-dimensional moiré crystal. *Phys. Rev. B*, 100:155416, Oct 2019.
- [21] Kha Tran, Galan Moody, Fengcheng Wu, Xiaobo Lu, Junho Choi, Kyoungwan Kim, Amritesh Rai, Daniel A. Sanchez, Jiamin Quan, Akshay Singh, Jacob Embley, André Zepeda, Marshall Campbell, Travis Autry, Takashi Taniguchi, Kenji Watanabe, Nanshu Lu, Sanjay K. Banerjee, Kevin L. Silverman, Suenne Kim, Emanuel Tutuc, Li Yang, Allan H. MacDonald, and Xiaoqin Li. Evidence for moiré excitons in van der waals heterostructures. *Nature*, 567(7746):71–75, 2019.
- [22] Alexander Epping, Luca Banszerus, Johannes Güttinger, Luisa Krückeberg, Kenji Watanabe, Takashi Taniguchi, Fabian Hassler, Bernd Beschoten, and Christoph Stampfer. Quantum transport through MoS₂ constrictions defined by photodoping. *Journal of Physics: Condensed Matter*, 30(20):205001, apr 2018.
- [23] Enxiu Wu, Yuan Xie, Qingzhou Liu, Xiaodong Hu, Jing Liu, Daihua Zhang, and Chongwu Zhou. Photoinduced doping to enable tunable and high-performance anti-ambipolar MoTe₂/MoS₂ heterotransistors. *ACS Nano*, 13(5):5430–5438, 2019. PMID: 30974935.
- [24] Sanghoon Kim, Sergey G. Menabde, and Min Seok Jang. Efficient photodoping of graphene in perovskite-graphene heterostructure. *Advanced Electronic Materials*, 5(3):1800940, 2019.
- [25] Enxiu Wu, Yuan Xie, Jing Zhang, Hao Zhang, Xiaodong Hu, Jing Liu, Chongwu Zhou, and Daihua Zhang. Dynamically controllable polarity modulation of MoTe₂ field-effect transistors through ultraviolet light and electrostatic activation. *Science Advances*, 5(5), 2019.
- [26] Xuyi Luo, Kraig Andrews, Tianjiao Wang, Arthur Bowman, Zhixian Zhou, and Ya-Qiong Xu. Reversible photo-induced doping in WSe₂ field effect transistors. *Nanoscale*, 11:7358–7363, 2019.
- [27] A. Rossi, D. Spirito, F. Bianco, S. Forti, F. Fabbri, H. Büch, A. Tredicucci, R. Krahn, and C. Coletti. Patterned tungsten disulfide/graphene heterostructures for efficient multifunctional optoelectronic devices. *Nanoscale*, 10:4332–4338, 2018.

-
- [28] Antonio Di Bartolomeo, Luca Genovese, Tobias Foller, Filippo Giubileo, Giuseppe Luongo, Luca Croin, Shi-Jun Liang, L K Ang, and Marika Schleberger. Electrical transport and persistent photoconductivity in monolayer MoS₂ phototransistors. *Nanotechnology*, 28(21):214002, 2017.
- [29] Young Duck Kim, Myung-Ho Bae, Jung-Tak Seo, Yong Seung Kim, Hakseong Kim, Jae Hong Lee, Joung Real Ahn, Sang Wook Lee, Seung-Hyun Chun, and Yun Daniel Park. Focused-laser-enabled p-n junctions in graphene field-effect transistors. *ACS Nano*, 7(7):5850–5857, 2013. PMID: 23782162.
- [30] Jorge Quereda, Talieh S Ghiasi, Caspar H van der Wal, and Bart J van Wees. Semiconductor channel-mediated photodoping in h-BN encapsulated monolayer MoSe₂ phototransistors. *2D Materials*, 6(2):025040, mar 2019.
- [31] Isidoro Martinez, Mário Ribeiro, Pablo Andres, Luis E. Hueso, Fèlix Casanova, and Farkhad G. Aliev. Photodoping-driven crossover in the low-frequency noise of MoS₂ transistors. *Phys. Rev. Applied*, 7:034034, Mar 2017.
- [32] Tao Liu, Du Xiang, Yue Zheng, Yanan Wang, Xinyun Wang, Li Wang, Jun He, Lei Liu, and Wei Chen. Nonvolatile and programmable photodoping in MoTe₂ for photoresist-free complementary electronic devices. *Advanced Materials*, 30(52):1804470, 2018.
- [33] Dong Li, Mingyuan Chen, Zhengzong Sun, Peng Yu, Zheng Liu, Pulickel M. Ajayan, and Zengxing Zhang. Two-dimensional non-volatile programmable p-n junctions. *Nature Nanotechnology*, 12:901–, June 2017.
- [34] Sung Hyun Kim, Sum-Gyun Yi, Myung Uk Park, ChangJun Lee, Myeongjin Kim, and Kyung-Hwa Yoo. Multilevel MoS₂ optical memory with photoresponsive top floating gates. *ACS Applied Materials & Interfaces*, 11(28):25306–25312, 2019. PMID: 31268292.
- [35] Natália P. Rezende, Alisson R. Cadore, Andreij C. Gadelha, Cítia L. Pereira, Vinícius Ornelas, Kenji Watanabe, Takashi Taniguchi, André S. Ferlauto, Angelo Malachias, Leonardo C. Campos, and Rodrigo G. Lacerda. Probing the electronic properties of monolayer MoS₂ via interaction with molecular hydrogen. *Advanced Electronic Materials*, 5(2):1800591, 2019.
- [36] Chung-Chiang Wu, Deep Jariwala, Vinod K. Sangwan, Tobin J. Marks, Mark C. Hersam, and Lincoln J. Lauhon. Elucidating the photoresponse of ultrathin MoS₂ field-effect transistors by scanning photocurrent microscopy. *The Journal of Physical Chemistry Letters*, 4(15):2508–2513, 2013.

-
- [37] Michele Buscema, Maria Barkelid, Val Zwiller, Herre S. J. van der Zant, Gary A. Steele, and Andres Castellanos-Gomez. Large and tunable photothermoelectric effect in single-layer MoS₂. *Nano Letters*, 13(2):358–363, 2013. PMID: 23301811.
- [38] Xiaodong Xu, Nathaniel M. Gabor, Jonathan S. Alden, Arend M. van der Zande, and Paul L. McEuen. Photo-thermoelectric effect at a graphene interface junction. *Nano Letters*, 10(2):562–566, 2010. PMID: 20038087.
- [39] Alexander E. Yore, Kirby K. H. Smithe, Sauraj Jha, Kyle Ray, Eric Pop, and A. K. M. Newaz. Large array fabrication of high performance monolayer MoS₂ photodetectors. *Applied Physics Letters*, 111(4):043110, 2017.
- [40] Yueh-Chun Wu, Cheng-Hua Liu, Shao-Yu Chen, Fu-Yu Shih, Po-Hsun Ho, Chun-Wei Chen, Chi-Te Liang, and Wei-Hua Wang. Extrinsic origin of persistent photoconductivity in monolayer MoS₂ field effect transistors. *Scientific Reports*, 5:11472–, June 2015.
- [41] Andres Castellanos-Gomez, Michele Buscema, Rianda Molenaar, Vibhor Singh, Laurens Janssen, Herre S J van der Zant, and Gary A Steele. Deterministic transfer of two-dimensional materials by all-dry viscoelastic stamping. *2D Materials*, 1(1):011002, 2014.